

<sup>1</sup> **Critical transitions and the fragmenting of global forests**

<sup>2</sup> **Leonardo A. Saravia<sup>1 3</sup>, Santiago R. Doyle<sup>1</sup>, Ben Bond-Lamberty<sup>2</sup>**

<sup>3</sup> 1. Instituto de Ciencias, Universidad Nacional de General Sarmiento, J.M. Gutierrez 1159 (1613), Los  
<sup>4</sup> Polvorines, Buenos Aires, Argentina.

<sup>5</sup> 2. Pacific Northwest National Laboratory, Joint Global Change Research Institute at the University of  
<sup>6</sup> Maryland–College Park, 5825 University Research Court #3500, College Park, MD 20740, USA

<sup>7</sup> 3. Corresponding author e-mail: lsaravia@ungs.edu.ar

<sup>8</sup> **Keywords:** Forest fragmentation, early warning signals, percolation, power-laws, MODIS, critical transitions

<sup>9</sup> **Running title:** Critical fragmentation in global forest

<sup>10</sup> **Abstract**

<sup>11</sup> 1. Forests provide critical habitat for many species, essential ecosystem services, and are coupled to  
<sup>12</sup> atmospheric dynamics through exchanges of energy, water and gases. One of the most important  
<sup>13</sup> changes produced in the biosphere is the replacement of forest areas with human dominated landscapes.  
<sup>14</sup> This usually leads to fragmentation, altering the sizes of patches, the structure and function of the  
<sup>15</sup> forest. Here we studied the distribution and dynamics of forest patch sizes at a global level, examining  
<sup>16</sup> signals of a critical transition from an unfragmented to a fragmented state.

<sup>17</sup> 2. We used MODIS vegetation continuous field to estimate the forest patches at a global level and de-  
<sup>18</sup> fined wide regions of connected forest across continents and big islands. We search for critical phase  
<sup>19</sup> transitions, where the system state of the forest changes suddenly at a critical point in time; this  
<sup>20</sup> implies an abrupt change in connectivity that causes an increased fragmentation level. We combined  
<sup>21</sup> five criteria to evaluate the closeness of the system to a fragmentation threshold, studying in particular  
<sup>22</sup> the distribution of forest patch sizes and the dynamics of the largest patch over the last sixteen years.

<sup>23</sup> 3. We found some necessary evidence that allows us to analyze fragmentation as a critical transition: all  
<sup>24</sup> regions followed a power-law distribution over the fifteen years. We also found that the Philippines  
<sup>25</sup> region probably went through a critical transition from a fragmented to an unfragmented state. Regions  
<sup>26</sup> with the highest deforestation rates—South America, Southeast Asia, Africa—all met the criteria to  
<sup>27</sup> be near a critical fragmentation threshold.

<sup>28</sup> 4. This implies that human pressures and climate forcings might trigger undesired effects of fragmentation,  
<sup>29</sup> such as species loss and degradation of ecosystems services, in these regions. The simple criteria  
<sup>30</sup> proposed here could be used as an early warning to estimate the distance to a fragmentation threshold  
<sup>31</sup> in forests around the globe.

## <sup>32</sup> Introduction

<sup>33</sup> Forests are one of the most important biomes on earth, providing habitat for a large proportion of species  
<sup>34</sup> and contributing extensively to global biodiversity (Crowther *et al.* 2015). In the previous century human  
<sup>35</sup> activities have influenced global bio-geochemical cycles (Bonan 2008; Canfield *et al.* 2010), with one of  
<sup>36</sup> the most dramatic changes being the replacement of 40% of Earth's formerly biodiverse land areas with  
<sup>37</sup> landscapes that contain only a few species of crop plants, domestic animals and humans (Foley *et al.* 2011).  
<sup>38</sup> These local changes have accumulated over time and now constitute a global forcing (Barnosky *et al.* 2012).  
<sup>39</sup> Another global scale forcing that is tied to habitat destruction is fragmentation, which is defined as the  
<sup>40</sup> division of a continuous habitat into separated portions that are smaller and more isolated. Fragmentation  
<sup>41</sup> produces multiple interwoven effects: reductions of biodiversity between 13% and 75%, decreasing forest  
<sup>42</sup> biomass, and changes in nutrient cycling (Haddad *et al.* 2015). The effects of fragmentation are not only  
<sup>43</sup> important from an ecological point of view but also that of human activities, as ecosystem services are deeply  
<sup>44</sup> influenced by the level of landscape fragmentation (Rudel *et al.* 2005; Angelsen 2010; Mitchell *et al.* 2015).

<sup>45</sup> Ecosystems have complex interactions between species and present feedbacks at different levels of organization  
<sup>46</sup> (Gilman *et al.* 2010), and external forcings can produce abrupt changes from one state to another, called  
<sup>47</sup> critical transitions (Scheffer *et al.* 2009). These abrupt state shifts cannot be linearly forecasted from past  
<sup>48</sup> changes, and are thus difficult to predict and manage (Scheffer *et al.* 2009). Such 'critical' transitions have  
<sup>49</sup> been detected mostly at local scales (Drake & Griffen 2010; Carpenter *et al.* 2011), but the accumulation of  
<sup>50</sup> changes in local communities that overlap geographically can propagate and theoretically cause an abrupt  
<sup>51</sup> change of the entire system at larger scales (Barnosky *et al.* 2012). Coupled with the existence of global  
<sup>52</sup> scale forcings, this implies the possibility that a critical transition could occur at a global scale (Rockstrom  
<sup>53</sup> *et al.* 2009; Folke *et al.* 2011).

<sup>54</sup> Complex systems can experience two general classes of critical transitions (Solé 2011). In so-called first  
<sup>55</sup> order transitions, a catastrophic regime shift that is mostly irreversible occurs because of the existence of  
<sup>56</sup> alternative stable states (Scheffer *et al.* 2001). This class of transitions is suspected to be present in a variety  
<sup>57</sup> of ecosystems such as lakes, woodlands, coral reefs (Scheffer *et al.* 2001), semi-arid grasslands (Bestelmeyer  
<sup>58</sup> *et al.* 2011), and fish populations (Vasilakopoulos & Marshall 2015). They can be the result of positive  
<sup>59</sup> feedback mechanisms (Villa Martín *et al.* 2015); for example, fires in some forest ecosystems were more  
<sup>60</sup> likely to occur in previously burned areas than in unburned places (Kitzberger *et al.* 2012).

<sup>61</sup> The other class of critical transitions are continuous or second order transitions (Solé & Bascompte 2006). In  
<sup>62</sup> these cases, there is a narrow region where the system suddenly changes from one domain to another, with

the change being continuous and in theory reversible. This kind of transitions were suggested to be present in tropical forests (Pueyo *et al.* 2010), semi-arid mountain ecosystems (McKenzie & Kennedy 2012), and tundra shrublands (Naito & Cairns 2015). The transition happens at a critical point where we can observe a distinctive spatial pattern: scale invariant fractal structures characterized by power law patch distributions (Stauffer & Aharony 1994). There are several processes that can convert a catastrophic transition to a second order transitions (Villa Martín *et al.* 2015). These include stochasticity, such as demographic fluctuations, spatial heterogeneities, and/or dispersal limitation. All these components are present in forest around the globe (Seidler & Plotkin 2006; Filotas *et al.* 2014; Fung *et al.* 2016), and thus continuous transitions might be more probable than catastrophic transitions. Moreover there is some evidence of recovery in some systems that supposedly suffered an irreversible transition produced by overgrazing (Zhang *et al.* 2005; Bestelmeyer *et al.* 2013) and desertification (Allington & Valone 2010).

The spatial phenomena observed in continuous critical transitions deal with connectivity, a fundamental property of general systems and ecosystems from forests (Ochoa-Quintero *et al.* 2015) to marine ecosystems (Leibold & Norberg 2004) and the whole biosphere (Lenton & Williams 2013). When a system goes from a fragmented to a connected state we say that it percolates (Solé 2011). Percolation implies that there is a path of connections that involves the whole system. Thus we can characterize two domains or phases: one dominated by short-range interactions where information cannot spread, and another in which long range interactions are possible and information can spread over the whole area. (The term “information” is used in a broad sense and can represent species dispersal or movement.) Thus, there is a critical “percolation threshold” between the two phases, and the system could be driven close to or beyond this point by an external force; climate change and deforestation are the main forces that could be the drivers of such a phase change in contemporary forests (Bonan 2008; Haddad *et al.* 2015). There are several applications of this concept in ecology: species’ dispersal strategies are influenced by percolation thresholds in three-dimensional forest structure (Solé *et al.* 2005), and it has been shown that species distributions also have percolation thresholds (He & Hubbell 2003). This implies that pushing the system below the percolation threshold could produce a biodiversity collapse (Bascompte & Solé 1996; Solé *et al.* 2004; Pardini *et al.* 2010); conversely, being in a connected state (above the threshold) could accelerate the invasion of forest into prairie (Loehle *et al.* 1996; Naito & Cairns 2015).

One of the main challenges with systems that can experience critical transitions—of any kind—is that the value of the critical threshold is not known in advance. In addition, because near the critical point a small change can precipitate a state shift of the system, they are difficult to predict. Several methods have been developed to detect if a system is close to the critical point, e.g. a deceleration in recovery from perturbations,

95 or an increase in variance in the spatial or temporal pattern (Hastings & Wysham 2010; Carpenter *et al.*  
96 2011; Boettiger & Hastings 2012; Dai *et al.* 2012).

97 The existence of a critical transition between two states has been established for forest at a global scale in  
98 different works (Hirotा *et al.* (2011); Staal *et al.* (2016); Wuyts *et al.* (2017)). It is generally believed that  
99 this constitutes a first order catastrophic transition. The regions where forest can grow are not distributed  
100 homogeneously, as there are demographic fluctuations in forest growth and disturbances produced by human  
101 activities. Due to new theoretical advances (Villa Martín *et al.* 2014, 2015) all these factors imply that if  
102 these were first order transitions they will be converted or observed as second order continuous transitions.  
103 Recently, percolation theory has been suggested as an explanation of power law forest fragments (Taubert  
104 *et al.* 2018). From this basis, we applied indices derived from second order transitions to global forest cover  
105 dynamics.

106 In this study, our objective is to look for evidence that forests around the globe are near continuous critical  
107 points that represent a fragmentation threshold. We use the framework of percolation to first evaluate if  
108 forest patch distribution at a continental scale is described by a power law distribution and then examine  
109 the fluctuations of the largest patch. The advantage of using data at a continental scale is that for very large  
110 systems the transitions are very sharp (Solé 2011) and thus much easier to detect than at smaller scales,  
111 where noise can mask the signals of the transition.

## 112 Methods

### 113 Study areas definition

114 We analyzed mainland forests at a continental scale, covering the whole globe, by delimiting land areas with  
115 a near-contiguous forest cover, separated with each other by large non-forested areas. Using this criterion,  
116 we delimited the following forest regions. In America, three regions were defined: South America temperate  
117 forest (SAT), subtropical and tropical forest up to Mexico (SAST), and USA and Canada forest (NA). Europe  
118 and North Asia were treated as one region (EUAS). The rest of the delimited regions were South-east Asia  
119 (SEAS), Africa (AF), and Australia (OC). We also included in the analysis islands larger than  $10^5\text{km}^2$ . The  
120 mainland region has the number 1 e.g. OC1, and the nearby islands have consecutive numeration (Appendix  
121 S4, figure S1-S6). We applied this criterion to delimit regions because we based our study on percolation  
122 theory that assumes some kind of connectivity in the study area (see below).

123 **Forest patch distribution**

124 We studied forest patch distribution in each defined area from 2000 to 2015 using the MODerate-resolution  
125 Imaging Spectroradiometer (MODIS) Vegetation Continuous Fields (VCF) Tree Cover dataset version 051  
126 (DiMiceli *et al.* 2015). This dataset is produced at a global level with a 231-m resolution, from 2000 onwards  
127 on an annual basis, the last available year was 2015. There are several definition of forest based on percent  
128 tree cover (Sexton *et al.* 2015); we choose a range from 20% to 40% threshold in 5% increments to convert  
129 the percentage tree cover to a binary image of forest and non-forest pixels. This range is centered in the  
130 definition used by the United Nations' International Geosphere-Biosphere Programme (Belward 1996), and  
131 studies of global fragmentation (Haddad *et al.* 2015) and includes the range used in other studies of critical  
132 transitions (Xu *et al.* 2016). Using this range we try to avoid the errors produced by low discrimination  
133 of MODIS VCF between forest and dense herbaceous vegetation at low forest cover and the saturation of  
134 MODIS VCF in dense forests (Sexton *et al.* 2013). We repeat all the analysis for this set of thresholds,  
135 except in some specific cases described below. Patches of contiguous forest were determined in the binary  
136 image by grouping connected forest pixels using a neighborhood of 8 forest units (Moore neighborhood).  
137 The MODIS VCF product defines the percentage of tree cover by pixel, but does not discriminate the type  
138 of trees so besides natural forest it includes plantations of tree crops like rubber, oil palm, eucalyptus and  
139 other managed stands (Hansen *et al.* 2014).

140 **Percolation theory**

141 A more in-depth introduction to percolation theory can be found elsewhere (Stauffer & Aharony 1994) and a  
142 review from an ecological point of view is available (Oborny *et al.* 2007). Here, to explain the basic elements  
143 of percolation theory we formulate a simple model: we represent our area of interest by a square lattice  
144 and each site of the lattice can be occupied—e.g. by forest—with a probability  $p$ . The lattice will be more  
145 occupied when  $p$  is greater, but the sites are randomly distributed. We are interested in the connection  
146 between sites, so we define a neighborhood as the eight adjacent sites surrounding any particular site. The  
147 sites that are neighbors of other occupied sites define a patch. When there is a patch that connects the  
148 lattice from opposite sides, it is said that the system percolates. When  $p$  is increased from low values, a  
149 percolating patch suddenly appears at some value of  $p$  called the critical point  $p_c$ .

150 Thus percolation is characterized by two well defined phases: the unconnected phase when  $p < p_c$  (called  
151 subcritical in physics), in which species cannot travel far inside the forest, as it is fragmented; in a general  
152 sense, information cannot spread. The second is the connected phase when  $p > p_c$  (supercritical), species

153 can move inside a forest patch from side to side of the area (lattice), i.e. information can spread over the  
154 whole area. Near the critical point several scaling laws arise: the structure of the patch that spans the area  
155 is fractal, the size distribution of the patches is power-law, and other quantities also follow power-law scaling  
156 (Stauffer & Aharony 1994).

157 The value of the critical point  $p_c$  depends on the geometry of the lattice and on the definition of the  
158 neighborhood, but other power-law exponents only depend on the lattice dimension. Close to the critical  
159 point, the distribution of patch sizes is:

160 (1)  $n_s(p_c) \propto s^{-\alpha}$

161 where  $n_s(p)$  is the number of patches of size  $s$ . The exponent  $\alpha$  does not depend on the details of the  
162 model and it is called universal (Stauffer & Aharony 1994). These scaling laws can be applied for landscape  
163 structures that are approximately random, or at least only correlated over short distances (Gastner *et al.*  
164 2009). In physics this is called “isotropic percolation universality class”, and corresponds to an exponent  
165  $\alpha = 2.05495$ . If we observe that the patch size distribution has another exponent it will not belong to this  
166 universality class and some other mechanism should be invoked to explain it. Percolation thresholds can also  
167 be generated by models that have some kind of memory (Hinrichsen 2000; Ódor 2004): for example, a patch  
168 that has been exploited for many years will recover differently than a recently deforested forest patch. In  
169 this case, the system could belong to a different universality class, or in some cases there is no universality,  
170 in which case the value of  $\alpha$  will depend on the parameters and details of the model (Corrado *et al.* 2014).

171 To illustrate these concepts, we conducted simulations with a simple forest model with only two states: forest  
172 and non-forest. This type of model is called a “contact process” and was introduced for epidemics (Harris  
173 1974), but has many applications in ecology (Solé & Bascompte 2006; Gastner *et al.* 2009). A site with forest  
174 can become extinct with probability  $e$ , and produce another forest site in a neighborhood with probability  
175  $c$ . We use a neighborhood defined by an isotropic power law probability distribution. We defined a single  
176 control parameter as  $\lambda = c/e$  and ran simulations for the subcritical fragmentation state  $\lambda < \lambda_c$ , with  $\lambda = 2$ ,  
177 near the critical point for  $\lambda = 2.5$ , and for the supercritical state with  $\lambda = 5$  (see supplementary data, gif  
178 animations).

179 **Patch size distributions**

180 We fitted the empirical distribution of forest patches calculated for each of the thresholds on the range we  
181 previously mentioned. We used maximum likelihood (Goldstein *et al.* 2004; Clauset *et al.* 2009) to fit four  
182 distributions: power-law, power-law with exponential cut-off, log-normal, and exponential. We assumed

183 that the patch size distribution is a continuous variable that was discretized by the remote sensing data  
184 acquisition procedure.

185 We set a minimal patch size ( $X_{min}$ ) at nine pixels to fit the patch size distributions to avoid artifacts at patch  
186 edges due to discretization (Weerman *et al.* 2012). Besides this hard  $X_{min}$  limit we set due to discretization,  
187 the power-law distribution needs a lower bound for its scaling behavior. This lower bound is also estimated  
188 from the data by maximizing the Kolmogorov-Smirnov (KS) statistic, computed by comparing the empirical  
189 and fitted cumulative distribution functions (Clauset *et al.* 2009). For the log-normal model we constrain  
190 the values of the  $\mu$  parameter to positive values, this parameter controls the mode of the distribution and  
191 when is negative most of the probability density of the distribution lies outside the range of the forest patch  
192 size data (Limpert *et al.* 2001).

193 To select the best model we calculated corrected Akaike Information Criteria ( $AIC_c$ ) and Akaike weights  
194 for each model (Burnham & Anderson 2002). Akaike weights ( $w_i$ ) are the weight of evidence in favor of  
195 model  $i$  being the actual best model given that one of the  $N$  models must be the best model for that set of  
196  $N$  models. Additionally, we computed a likelihood ratio test (Vuong 1989; Clauset *et al.* 2009) of the power  
197 law model against the other distributions. We calculated bootstrapped 95% confidence intervals (Crawley  
198 2012) for the parameters of the best model, using the bias-corrected and accelerated (BCa) bootstrap (Efron  
199 & Tibshirani 1994) with 10000 replications.

## 200 Largest patch dynamics

201 The largest patch is the one that connects the highest number of sites in the area. This has been used  
202 extensively to indicate fragmentation (Gardner & Urban 2007; Ochoa-Quintero *et al.* 2015). The relation  
203 of the size of the largest patch  $S_{max}$  to critical transitions has been extensively studied in relation to  
204 percolation phenomena (Stauffer & Aharony 1994; Bazant 2000; Botet & Ploszajczak 2004), but is seldom  
205 used in ecological studies (for an exception see Gastner *et al.* (2009)). When the system is in a connected  
206 state ( $p > p_c$ ) the landscape is almost insensitive to the loss of a small fraction of forest, but close to the  
207 critical point a minor loss can have important effects (Solé & Bascompte 2006; Oborny *et al.* 2007), because  
208 at this point the largest patch will have a filamentary structure, i.e. extended forest areas will be connected  
209 by thin threads. Small losses can thus produce large fluctuations.

210 One way to evaluate the fragmentation of the forest is to calculate the proportion of the largest patch against  
211 the total area (Keitt *et al.* 1997). The total area of the regions we are considering (Appendix S4, figures  
212 S1-S6) may not be the same as the total area that the forest could potentially occupy, and thus a more

213 accurate way to evaluate the weight of  $S_{max}$  is to use the total forest area, which can be easily calculated  
214 by summing all the forest pixels. We calculate the proportion of the largest patch for each year, dividing  
215  $S_{max}$  by the total forest area of the same year:  $RS_{max} = S_{max} / \sum_i S_i$ . This has the effect of reducing the  
216  $S_{max}$  fluctuations produced due to environmental or climatic changes influences in total forest area. When  
217 the proportion  $RS_{max}$  is large (more than 60%) the largest patch contains most of the forest so there are  
218 fewer small forest patches and the system is probably in a connected phase. Conversely, when it is low (less  
219 than 20%), the system is probably in a fragmented phase (Saravia & Momo 2017). To define if a region will  
220 be in a connected or unconnected state we used the  $RS_{max}$  of the highest (i.e., most conservative) threshold  
221 of 40%, that represent the most dense area of forest within our chosen range. We assume that there are  
222 two alternative states for the critical transition—the forest could be fragmented or unfragmented. If  $RS_{max}$   
223 is a good indicator of the fragmentation state of the forest its distribution of frequencies should be bimodal  
224 (Bestelmeyer *et al.* 2011), so we apply the Hartigan's dip test that measures departures from unimodality  
225 (Hartigan & Hartigan 1985).

226 The  $RS_{max}$  is a useful qualitative index that does not tell us if the system is near or far from the critical  
227 transition; this can be evaluated using the temporal fluctuations. We calculate the fluctuations around the  
228 mean with the absolute values  $\Delta S_{max} = S_{max}(t) - \langle S_{max} \rangle$ , using the proportions of  $RS_{max}$ . To characterize  
229 fluctuations we fitted three empirical distributions: power-law, log-normal, and exponential, using the same  
230 methods described previously. We expect that large fluctuation near a critical point have heavy tails (log-  
231 normal or power-law) and that fluctuations far from a critical point have exponential tails, corresponding to  
232 Gaussian processes (Rooij *et al.* 2013). As the data set spans 16 years, it is probable that we will not have  
233 enough power to reliably detect which distribution is better (Clauset *et al.* 2009). To improve this we used  
234 the same likelihood ratio test we used previously (Vuong 1989; Clauset *et al.* 2009); if the p-values obtained  
235 to compare the best distribution against the others are not significant we concluded that there is not enough  
236 data to decide which is the best model. We generated animated maps showing the fluctuations of the two  
237 largest patches at 30% threshold, to aid in the interpretations of the results.

238 A robust way to detect if the system is near a critical transition is to analyze the increase in variance of the  
239 density (Benedetti-Cecchi *et al.* 2015)—in our case density is the total forest cover divided by the area. It  
240 has been demonstrated that the variance increase in the density of patches appears when the system is very  
241 close to the transition (Corrado *et al.* 2014), and thus practically it does not constitute an early warning  
242 indicator. An alternative is to analyze the variance of the fluctuations of the largest patch  $\Delta S_{max}$ : the  
243 maximum is attained at the critical point but a significant increase occurs well before the system reaches the  
244 critical point (Corrado *et al.* 2014; Saravia & Momo 2017). In addition, before the critical fragmentation,

245 the skewness of the distribution of  $\Delta S_{max}$  should be negative, implying that fluctuations below the average  
246 are more frequent. We characterized the increase in the variance using quantile regression: if variance is  
247 increasing the slopes of upper or/and lower quartiles should be positive or negative.

248 All statistical analyses were performed using the GNU R version 3.3.0 (R Core Team 2015), to fit the  
249 distributions of patch sizes we used the Python package powerlaw (Alstott *et al.* 2014). For the quantile  
250 regressions we used the R package quantreg (Koenker 2016). Image processing was done in MATLAB r2015b  
251 (The Mathworks Inc.). The complete source code for image processing and statistical analysis, and the patch  
252 size data files are available at figshare <http://dx.doi.org/10.6084/m9.figshare.4263905>.

## 253 Results

254 The figure 1 shows an example of the distribution of the biggest 200 patches for years 2000 and 2014. This  
255 distribution is highly variable; the biggest patch usually maintains its spatial location, but sometimes it  
256 breaks and then big fluctuations in its size are observed, as we will analyze below. Smaller patches can  
257 merge or break more easily so they enter or leave the list of 200, and this is why there is a color change  
258 across years.

259 The power law distribution was selected as the best model in 99% of the cases (Figure S7). In a small  
260 number of cases (1%) the power law with exponential cutoff was selected, but the value of the parameter  $\alpha$   
261 was similar by  $\pm 0.03$  to the pure power law (Table S1, and model fit data table). Additionally the patch size  
262 where the exponential tail begins is very large, and thus we used the power law parameters for these cases  
263 (region EUAS3,SAST2). In finite-size systems the favored model should be the power law with exponential  
264 cut-off, because the power-law tails are truncated to the size of the system (Stauffer & Aharony 1994). This  
265 implies that differences between the two kinds of power law models should be small. We observe this effect:  
266 when the pure power-law model is selected as the best model the likelihood ratio test shows that in 64% of  
267 the cases the differences with power law with exponential cutoff are not significant ( $p\text{-value}>0.05$ ); in these  
268 cases the differences between the fitted  $\alpha$  for both models are less than 0.001. Instead the likelihood ratio  
269 test clearly differentiates the power law model from the exponential model (100% cases  $p\text{-value}<0.05$ ), and  
270 the log-normal model (90% cases  $p\text{-value}<0.05$ ).

271 The global mean of the power-law exponent  $\alpha$  is 1.967 and the bootstrapped 95% confidence interval is  
272 1.964 - 1.970. The global values for each threshold are different, because their confidence intervals do not  
273 overlap, and their range goes from 1.90 to 2.01 (Table S1). Analyzing the biggest regions (Figure 1, Table  
274 S2) the northern hemisphere regions (EUAS1 & NA1) have similar values of  $\alpha$  (1.97, 1.98), pantropical areas

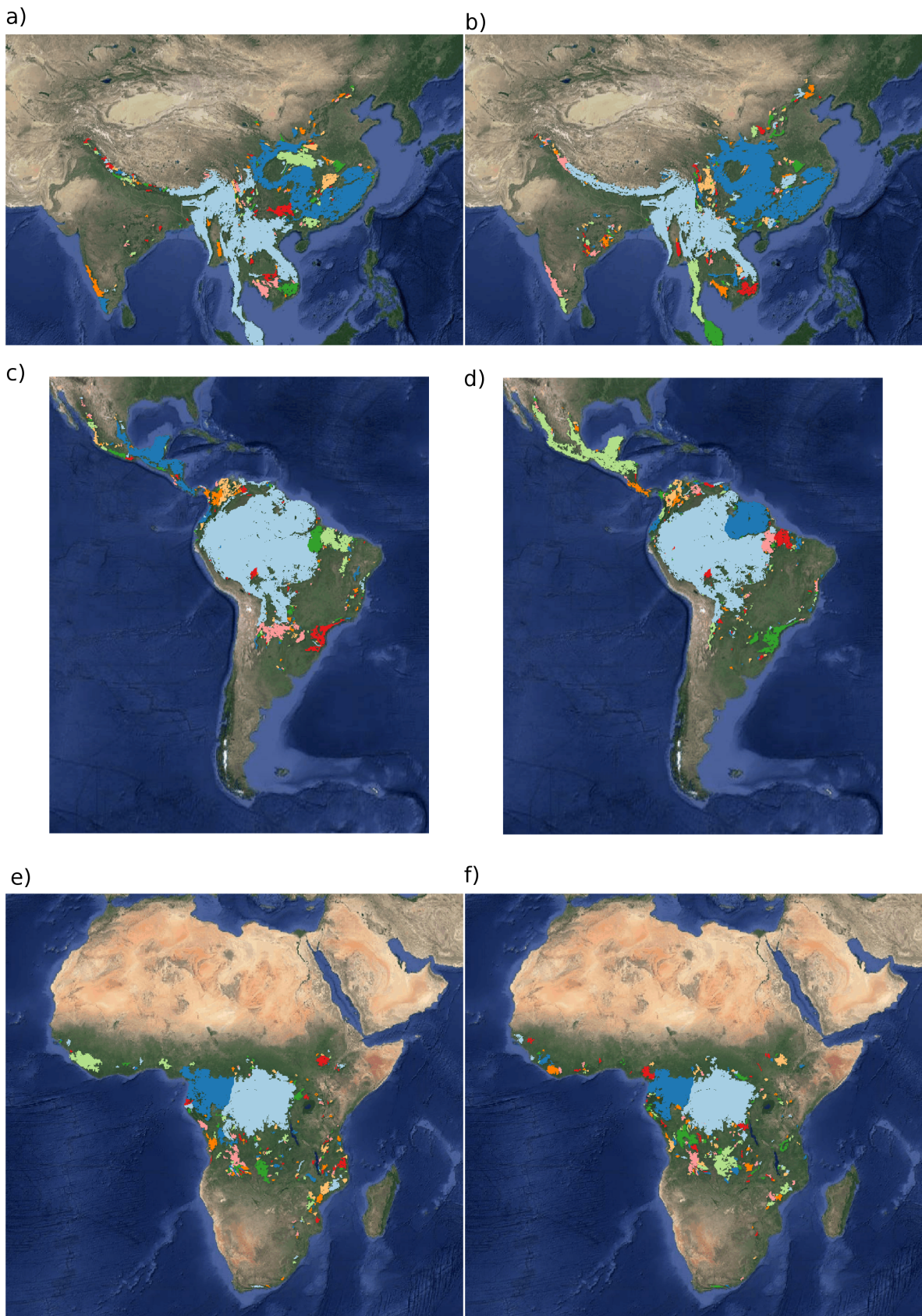


Figure 1: Forest patch distributions for continental regions for the years 2000 and 2014. The images are the 200 biggest patches, shown at a coarse pixel scale of 2.5 km. The regions are: a) & b) southeast Asia; c) & d) South America subtropical and tropical and e) & f) Africa mainland, for the years 2000 and 2014 respectively. The color palette was chosen to discriminate different patches and does not represent patch size.

275 have different  $\alpha$  with greatest values for South America (SAST1, 2.01) and in descending order Africa (AF1,  
 276 1.946) and Southeast Asia (SEAS1, 1.895). With greater  $\alpha$  the fluctuations of patch sizes are lower and vice  
 277 versa (Newman 2005).

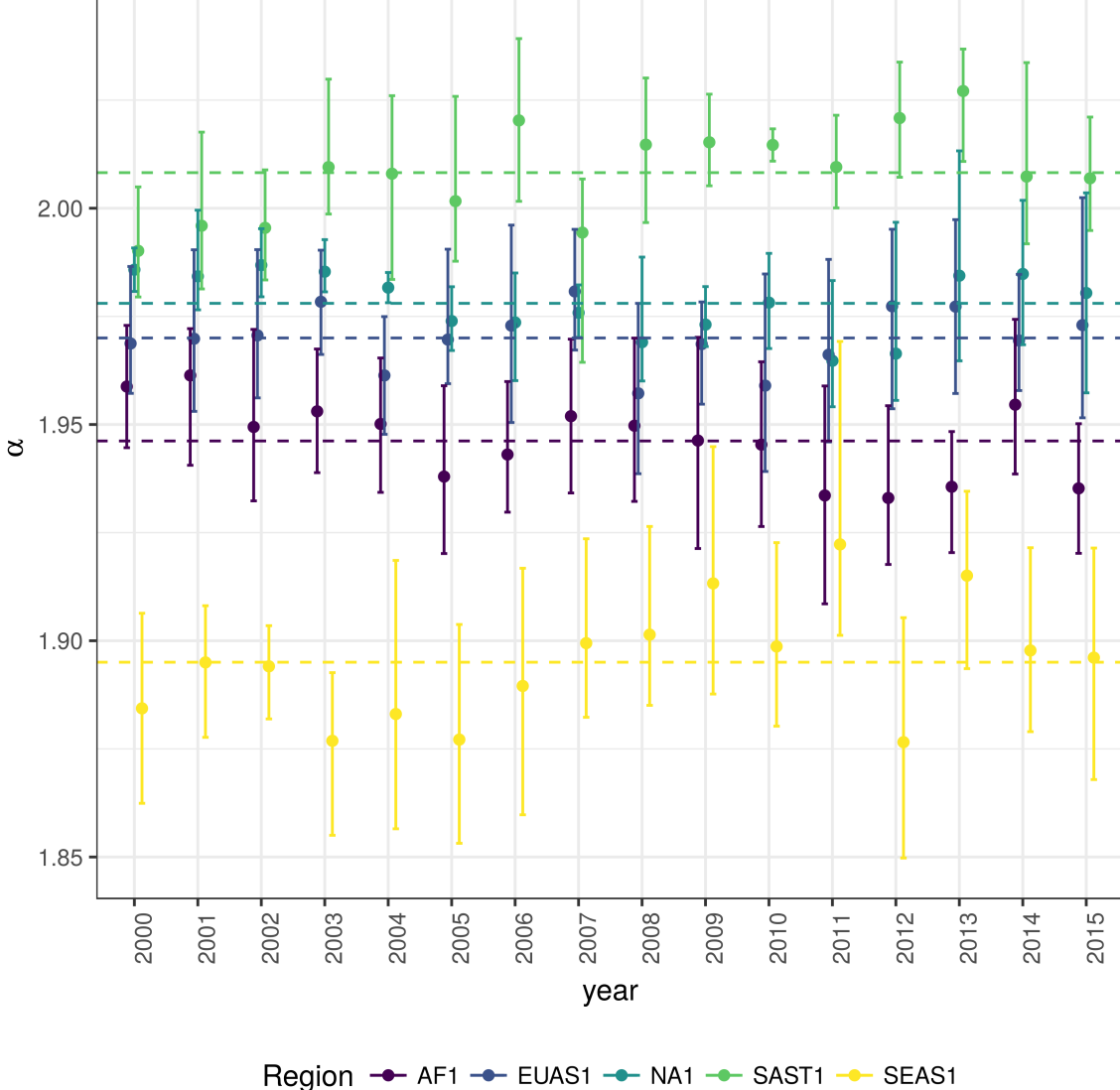


Figure 2: Power law exponents ( $\alpha$ ) of forest patch distributions for regions with total forest area  $> 10^7$  km $^2$ . Dashed horizontal lines are the means by region, with 95% confidence interval error bars estimated by bootstrap resampling. The regions are AF1: Africa mainland, EUAS1: Eurasia mainland, NA1: North America mainland, SAST1: South America subtropical and tropical, SEAS1: Southeast Asia mainland.

278 We calculated the total areas of forest and the largest patch  $S_{max}$  by year for different thresholds, and as  
 279 expected these two values increase for smaller thresholds (Table S3). We expect fewer variations in the  
 280 largest patch relative to total forest area  $RS_{max}$  (Figure S9); in ten cases it stayed near or higher than 60%  
 281 (EUAS2, NA5, OC2, OC3, OC4, OC5, OC6, OC8, SAST1, SAT1) over the 25-35 range or more. In four

282 cases it stayed around 40% or less, at least over the 25-30% range (AF1, EUAS3, OC1, SAST2), and in six  
 283 cases there is a crossover from more than 60% to around 40% or less (AF2, EUAS1, NA1, OC7, SEAS1,  
 284 SEAS2). This confirms the criteria of using the most conservative threshold value of 40% to interpret  $RS_{max}$   
 285 with regard to the fragmentation state of the forest. The frequency of  $RS_{max}$  showed bimodality (Figure 3)  
 286 and the dip test rejected unimodality ( $D = 0.0416$ ,  $p$ -value = 0.0003), which also implies that  $RS_{max}$  is a  
 287 good index to study the fragmentation state of the forest.

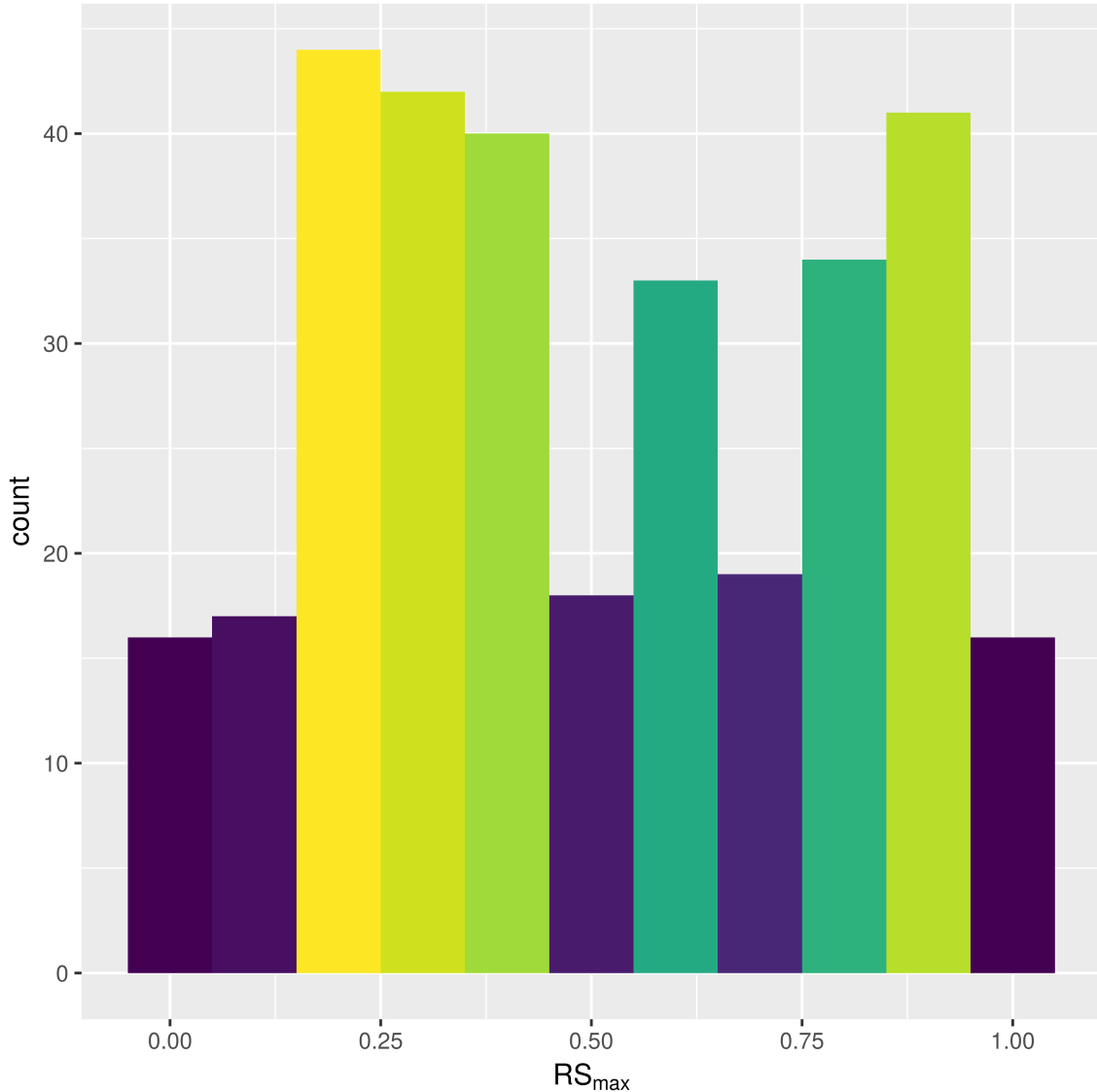


Figure 3: Frequency distribution of Largest patch proportion relative to total forest area  $RS_{max}$  calculated using a threshold of 40% of forest in each pixel to determine patches. Bimodality is observed and confirmed by the dip test ( $D = 0.0416$ ,  $p$ -value = 0.0003). This indicates the existence of two states needed for a critical transition.

288 The  $RS_{max}$  for regions with more than  $10^7$  km<sup>2</sup> of forest is shown in figure 4. South America tropical and

289 subtropical (SAST1) is the only region with an average close to 60%, the other regions are below 30%. Eurasia  
290 mainland (EUAS1) has the lowest value near 20%. For regions with less total forest area (Figure S10, Table  
291 S3), Great Britain (EUAS3) has the lowest proportion less than 5%, Java (OC7) and Cuba (SAST2) are  
292 under 25%, while other regions such as New Guinea (OC2), Malaysia/Kalimantan (OC3), Sumatra (OC4),  
293 Sulawesi (OC5) and South New Zealand (OC6) have a very high proportion (75% or more). Philippines  
294 (SEAS2) seems to be a very interesting case because it seems to be under 30% until the year 2007, fluctuates  
295 around 30% in years 2008-2010, then jumps near 60% in 2011-2013 and then falls again to 30%, this seems  
296 an example of a transition from a fragmented state to a unfragmented one (figure S10).

297 We analyzed the distributions of fluctuations of the largest patch relative to total forest area  $\Delta RS_{max}$  and  
298 the fluctuations of the largest patch  $\Delta S_{max}$ . Although the Akaike criteria identified different distributions  
299 as the best, in most cases the Likelihood ratio test was not significant and we are not able, from these data,  
300 to determine with confidence which is the best distribution. In only one case was the distribution selected  
301 by the Akaike criteria confirmed as the correct model for relative and absolute fluctuations (Table S4).

302 The animations of the two largest patches (see supplementary data, largest patch gif animations) qualitatively  
303 shows the nature of fluctuations and if the state of the forest is connected or not. If the largest patch is  
304 always the same patch over time, the forest is probably not fragmented; this happens for regions with  $RS_{max}$   
305 of more than 40% such as AF2 (Madagascar), EUAS2 (Japan), NA5 (Newfoundland) and OC3 (Malaysia).

306 In regions with  $RS_{max}$  between 40% and 30% the identity of the largest patch could change or stay the same  
307 in time. For OC7 (Java) the largest patch changes and for AF1 (Africa mainland) it stays the same. Only for  
308 EUAS1 (Eurasia mainland) did we observe that the two largest patches are always the same, implying that  
309 this region is probably composed of two independent domains and should be sub-divided in future studies.  
310 The regions with  $RS_{max}$  less than 25% included SAST2 (Cuba) and EUAS3 (Great Britain); in these cases  
311 the always-changing largest patch reflects their fragmented state. In the case of SEAS2 (Philippines) a  
312 transition is observed, with the identity of the largest patch first variable, and then constant after 2010.

313 The results of quantile regressions are almost identical for  $\Delta RS_{max}$  and  $\Delta S_{max}$  (table S5). Among the biggest  
314 regions, Africa (AF1) has a similar pattern across thresholds but only the 30% threshold is significant; the  
315 upper and lower quantiles have significant negative slopes, but the lower quantile slope is lower, implying  
316 that negative fluctuations and variance are increasing (Figure 5). Eurasia mainland (EUAS1) has significant  
317 slopes at 20%, 30% and 40% thresholds but the patterns are different at 20% variance is decreasing, at 30%  
318 and 40% only is increasing. Thus the variation of the most dense portion of the largest patch is increasing  
319 within a limited range. North America mainland (NA1) exhibits the same pattern at 20%, 25% and 30%  
320 thresholds: a significant lower quantile with positive slope, implying decreasing variance. South America

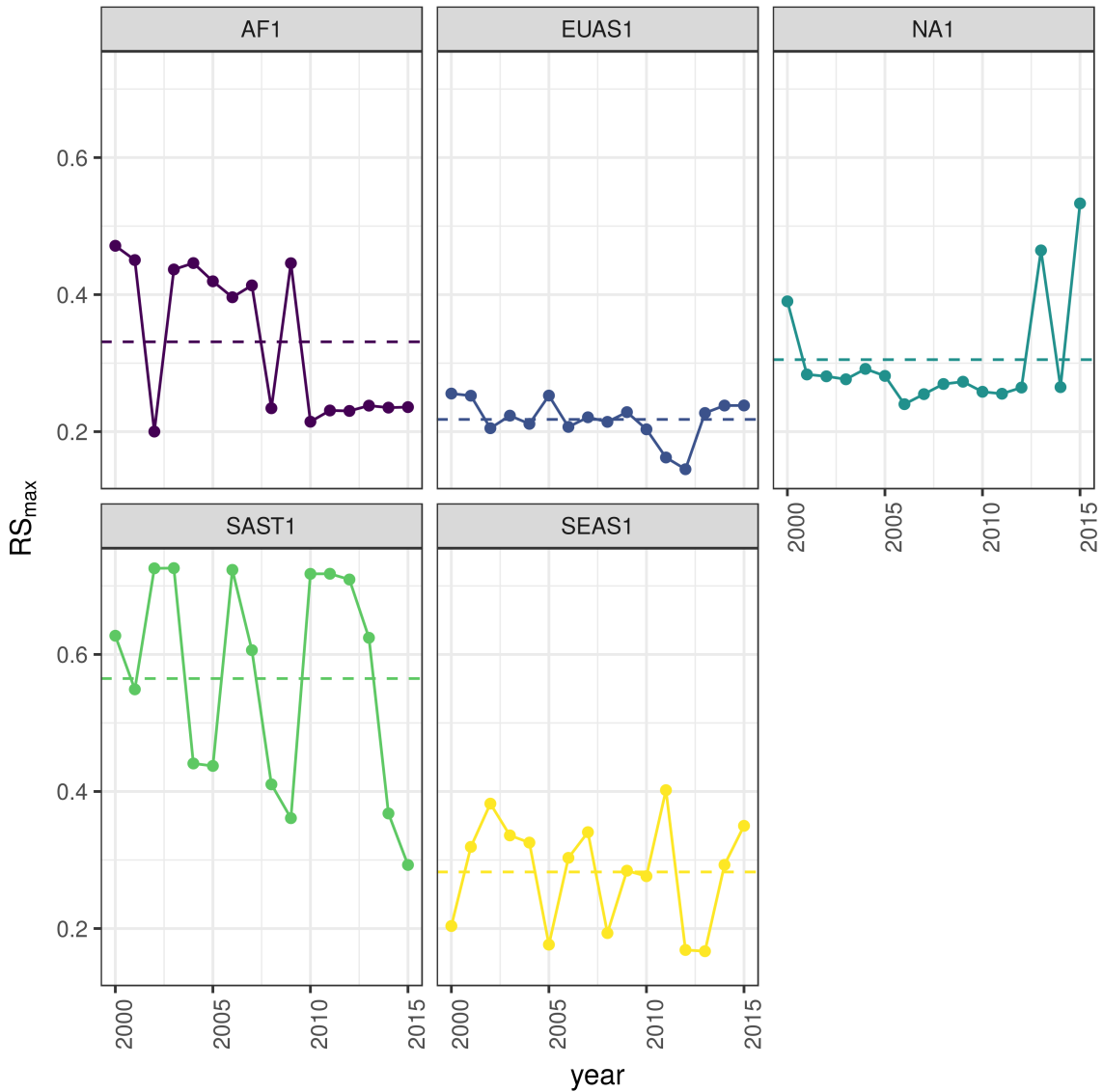


Figure 4: Largest patch proportion relative to total forest area  $RS_{max}$ , for regions with total forest area  $> 10^7 \text{ km}^2$ . We show here the  $RS_{max}$  calculated using a threshold of 40% of forest in each pixel to determine patches. Dashed lines are averages across time. The regions are AF1: Africa mainland, EUAS1: Eurasia mainland, NA1: North America mainland, SAST1: South America tropical and subtropical, SEAS1: Southeast Asia mainland.

321 tropical and subtropical (SAST1) have significant lower quantile with a negative slope at 25% and 30%  
322 thresholds indicating an increase in variance. SEAS1 has an upper quantile with positive slope significant  
323 for 25% threshold, also indicating an increasing variance. The other regions, with forest area smaller than  
324  $10^7 \text{ km}^2$  are shown in figure S11 and table S5. Philippines (SEAS2) is an interesting case: the slopes of lower  
325 quantiles are positive for thresholds 20% and 25%, and the upper quantile slopes are positive for thresholds  
326 30% and 40%; thus variance is decreasing at 20%-25% and increasing at 30%-40%.

327 The conditions that indicate that a region is near a critical fragmentation threshold are that patch size  
328 distributions follow a power law; variance of  $\Delta RS_{max}$  is increasing in time; and skewness is negative. All  
329 these conditions must happen at the same time at least for one threshold. When the threshold is higher more  
330 dense regions of the forest are at risk. This happens for Africa mainland (AF1), Eurasia mainland(EUAS1),  
331 Japan (EUAS2), Australia mainland (OC1), Malaysia/Kalimantan (OC3), Sumatra (OC4), South America  
332 tropical & subtropical (SAST1), Cuba (SAST2), Southeast Asia, Mainland (SEAS1).

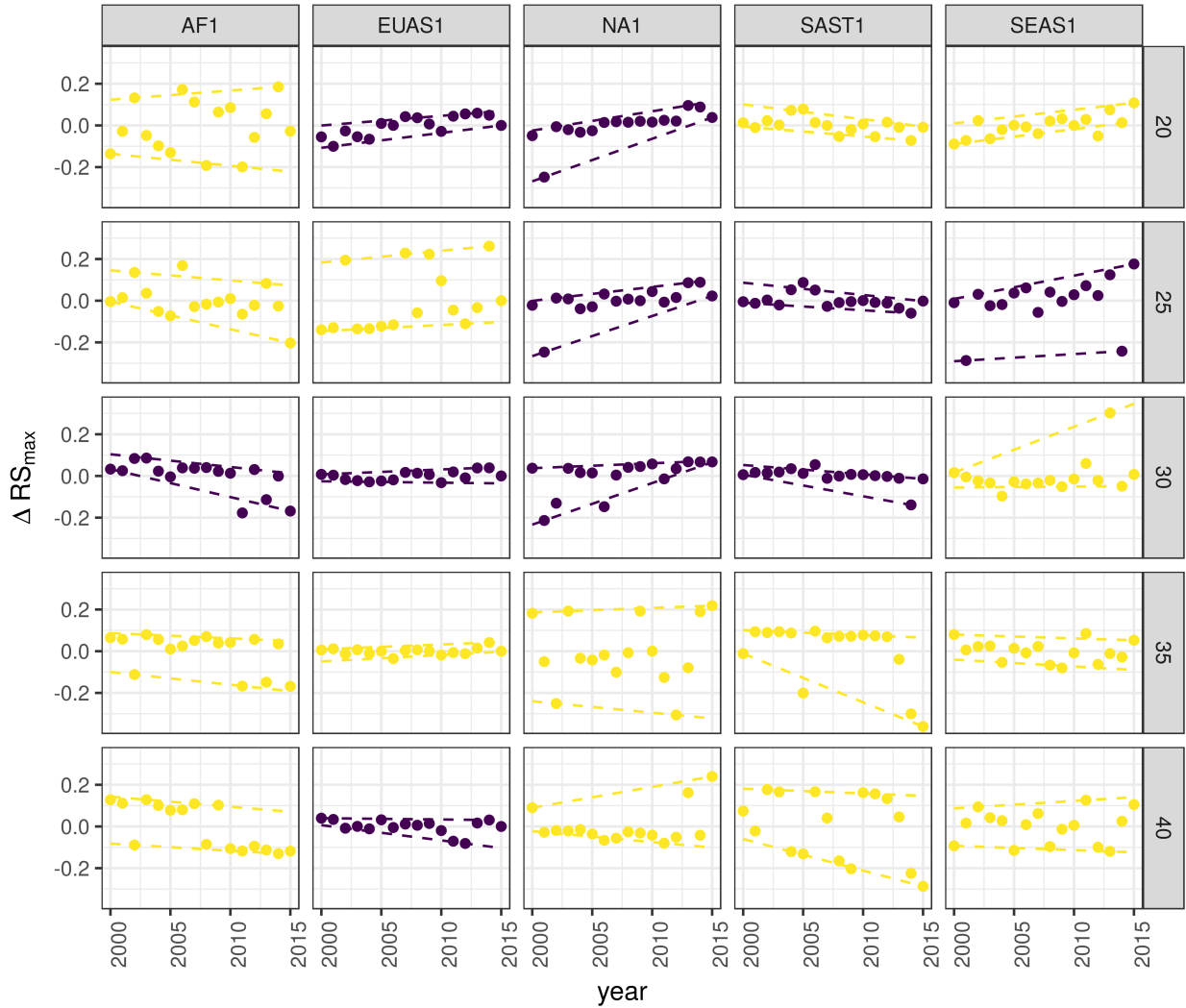


Figure 5: Largest patch fluctuations for regions with total forest area  $> 10^7 \text{ km}^2$  across years. The patch sizes are relative to the total forest area of the same year. Dashed lines are 90% and 10% quantile regressions, to show if fluctuations were increasing; purple (dark) panels have significant slopes. The regions are AF1: Africa mainland, EUAS1: Eurasia mainland, NA1: North America mainland, SAST1: South America tropical and subtropical, SEAS1: Southeast Asia mainland.

Table 1: Regions and indicators of closeness to a critical fragmentation point. Where:  $RS_{max}$  is the largest patch divided by the total forest area; Threshold is the value used to calculate patches from the MODIS VCF pixels;  $\Delta RS_{max}$  are the fluctuations of  $RS_{max}$  around the mean and the increase or decrease in the variance was estimated using quantile regressions; skewness was calculated for  $RS_{max}$ . NS means the results were non-significant. The conditions that determine the closeness to a fragmentation point are: increasing variance of  $\Delta RS_{max}$  and negative skewness.  $RS_{max}$  indicates if the forest is unfragmented ( $>0.6$ ) or fragmented ( $<0.3$ ).

Region	Description	$RS_{max}$	Threshold	Variance of $\Delta RS_{max}$	Skewness
AF1	Africa mainland	0.33	30	Increase	-1.4653
AF2	Madagascar	0.48	20	Increase	0.7226
EUAS1	Eurasia, mainland	0.22	20	Decrease	-0.4814
EUAS1			30	Increase	0.3113
EUAS1			40	Increase	-1.2790
EUAS2	Japan	0.94	35	Increase	-0.3913
EUAS2			40	Increase	-0.5030
EUAS3	Great Britain	0.03	40	NS	
NA1	North America, mainland	0.31	20	Decrease	-2.2895
NA1			25	Decrease	-2.4465
NA1			30	Decrease	-1.6340
NA5	Newfoundland	0.54	40	NS	
OC1	Australia, Mainland	0.36	30	Increase	0.0920
OC1			35	Increase	-0.8033
OC2	New Guinea	0.96	25	Decrease	-0.1003
OC2			30	Decrease	0.1214
OC2			35	Decrease	-0.0124
OC3	Malaysia/Kalimantan	0.92	35	Increase	-1.0147
OC3			40	Increase	-1.5649
OC4	Sumatra	0.84	20	Increase	-1.3846
OC4			25	Increase	-0.5887
OC4			30	Increase	-1.4226
OC5	Sulawesi	0.82	40	NS	
OC6	New Zealand South Island	0.75	40	Increase	0.3553
OC7	Java	0.16	40	NS	
OC8	New Zealand North Island	0.64	40	NS	
SAST1	South America, Tropical and Subtropical forest	0.56	25	Increase	1.0519
SAST1			30	Increase	-2.7216
SAST2	Cuba	0.15	20	Increase	0.5049
SAST2			25	Increase	1.7263
SAST2			30	Increase	0.1665
SAST2			40	Increase	-0.5401
SAT1	South America, Temperate forest	0.54	25	Decrease	0.1483
SAT1			30	Decrease	-1.6059
SAT1			35	Decrease	-1.3809
SEAS1	Southeast Asia, Mainland	0.28	25	Increase	-1.3328
SEAS2	Philippines	0.33	20	Decrease	-1.6373
SEAS2			25	Decrease	-0.6648
SEAS2			30	Increase	0.1517

Region	Description	$RS_{max}$	Threshold	Variance of $\Delta RS_{max}$	Skewness
SEAS2			40	Increase	1.5996

## 333 Discussion

334 We found that the forest patch distribution of all regions of the world, spanning tropical rainforests, boreal  
 335 and temperate forests, followed power laws spanning seven orders of magnitude. Power laws have previously  
 336 been found for several kinds of vegetation, but never at global scales as in this study. Moreover, the range  
 337 of the estimated power law exponents is relatively narrow (1.90 - 2.01), even though we tested a variety  
 338 of different thresholds levels. This suggests the existence of one unifying mechanism, or perhaps different  
 339 mechanisms that act in the same way in different regions, affecting forest spatial structure and dynamics.

340 Several mechanisms have been proposed for the emergence of power laws in forests. The first is related self  
 341 organized criticality (SOC), when the system is driven by its internal dynamics to a critical state; this has  
 342 been suggested mainly for fire-driven forests (Zinck & Grimm 2009; Hantson *et al.* 2015). Real ecosystems  
 343 do not seem to meet the requirements of SOC dynamics (Pueyo *et al.* 2010; McKenzie & Kennedy 2012),  
 344 however, because they have both endogenous and exogenous controls, are non-homogeneous, and do not  
 345 have a separation of time scales (Solé *et al.* 2002; Solé & Bascompte 2006). A second possible mechanism,  
 346 suggested by Pueyo *et al.* (2010), is isotropic percolation: when a system is near the critical point, the  
 347 power law structures arise. This is equivalent to the random forest model that we explained previously, and  
 348 requires the tuning of an external environmental condition to carry the system to this point. We did not  
 349 expect forest growth to be a random process at local scales, but it is possible that combinations of factors  
 350 cancel out to produce seemingly random forest dynamics at large scales. In this case we should have observed  
 351 power laws in a limited set of situations that coincide with a critical point, but instead we observed pervasive  
 352 power law distributions. Thus isotropic percolation does not seem likely to be the mechanism that produces  
 353 the observed distributions. A third possible mechanism is facilitation (Manor & Shnerb 2008; Irvine *et al.*  
 354 2016): a patch surrounded by forest will have a smaller probability of being deforested or degraded than  
 355 an isolated patch. The model of Scanlon *et al.* (2007) showed an  $\alpha = 1.34$  which is different from our  
 356 results (1.90 - 2.01 range). Another model but with three states (tree/non-tree/degraded), including local  
 357 facilitation and grazing, was also used to obtain power laws patch distributions without external tuning, and  
 358 exhibited deviations from power laws at high grazing pressures (Kéfi *et al.* 2007). The values of the power  
 359 law exponent  $\alpha$  obtained for this model are dependent on the intensity of facilitation: when facilitation is  
 360 more intense the exponent is higher, but the maximal values they obtained are still lower than the ones we

361 observed. The interesting point is that the value of the exponent is dependent on the parameters, and thus  
362 the observed  $\alpha$  might be obtained with some parameter combination.

363 The existence of possible critical transitions in forests, mainly in neotropical forest to savanna, is a matter  
364 of intense investigation, with the transitions generally thought to be first order or discontinuous transitions.  
365 Here, however, we found power laws in forest patch distributions, implying (i.e., a necessary but not a  
366 sufficient condition) a second order or continuous transition. A power law patch distribution can be indicative  
367 of a critical transition if it is present in a narrow range of conditions; conversely, if it is not found, the existence  
368 of a critical transition cannot be discarded. New research (Villa Martín *et al.* 2014, 2015) has suggested  
369 that first order transitions do not even exist when the system is (i) spatially heterogeneous and (ii) exhibits  
370 internal and external stochastic fluctuations, as in forests. Thus the application of indices based on second  
371 order transitions seems to be justified.

372 It has been suggested that a combination of spatial and temporal indicators could more reliably detect critical  
373 transitions (Kéfi *et al.* 2014). In this study, we combined five criteria to evaluate the closeness of the system  
374 to a fragmentation threshold. Two of them were spatial: the forest patch size distribution, and the proportion  
375 of the largest patch relative to total forest area  $RS_{max}$ . The other three were the distribution of temporal  
376 fluctuations in the largest patch size, the trend in the variance, and the skewness of the fluctuations. One  
377 of them: the distribution of temporal fluctuations  $\Delta RS_{max}$  can not be applied with our temporal resolution  
378 due to the difficulties of fitting and comparing heavy tailed distributions. The combination of the remaining  
379 four gives us an increased degree of confidence about the system being close to a critical transition.

380 Monitoring the biggest patches using  $RS_{max}$  is also important regardless of the existence or not of critical  
381 transitions.  $RS_{max}$  is relative to total forest area thus it could be used to compare regions with a different  
382 extension of forests and as the total area of forest also changes with different environmental conditions,  
383 e.g. this could be used to compare forest from different latitudes. Moreover, the areas covered by  $S_{max}$   
384 across regions contain most of the intact forest landscapes defined by Potapov *et al.* (2008b), and thus  
385  $RS_{max}$  is a relatively simple way to evaluate the risk in these areas.

386 This analysis is at scale of continents so it is in fact a macrosystems analysis (Heffernan *et al.* 2014), in  
387 which it is important to link local processes with resulting larger-scale (here, continental) patterns. Here, we  
388 identified macro-scale dynamical patterns that deserve attention. To link these patterns across scales requires  
389 a substantial amount of investigation, probably performing the same analysis for smaller regions that identify  
390 more clearly which kind of forest and processes are locally involved. We know that the same procedure could  
391 be applied to local scales because the patch distributions are power laws; power law distributions are self-

392 similar, or invariant to scale changes. Thus unless power law distribution are broken we could apply the  
393 same methodology to more local scales.

394 South America tropical and subtropical (SAST1), Southeast Asia mainland (SEAS1) and Africa mainland  
395 (AF1) met all criteria at least for one threshold; these regions generally experience the biggest rates of  
396 deforestation with a significant increase in loss of forest (Hansen *et al.* 2013). From our point of view the  
397 most critical region is Southeast Asia, because the proportion of the largest patch relative to total forest  
398 area  $RS_{max}$  was 28%. This suggests that Southeast Asia's forests are the most fragmented, and thus its  
399 flora and fauna the most endangered. Due to the criteria we adopted to define regions, we could not detect  
400 the effect of conservation policies applied at a country level, e.g. the Natural Forest Conservation Program  
401 in China, which has produced an 1.6% increase in forest cover and net primary productivity over the last 20  
402 years (Viña *et al.* 2016). Indonesia and Malaysia (OC3) both are countries with hight deforestation rates  
403 (Hansen *et al.* 2013); Sumatra (OC4) is the biggest island of Indonesia and where most deforestation occurs.  
404 Both regions show a high  $RS_{max}$  greater than 60%, and thus the forest is in an unfragmented state, but  
405 they met all other criteria, meaning that they are approaching a transition if the actual deforestation rates  
406 continue. At present our indices are qualitative but we expect to develop them in a more quantitative way  
407 to predict how many years would be needed to complete a critical transition if actual forest loss rates are  
408 maintained.

409 The Eurasian mainland region (EUAS1) is an extensive area with mainly temperate and boreal forest, and a  
410 combination of forest loss due to fire (Potapov *et al.* 2008a) and forestry. The biggest country is Russia that  
411 experienced the biggest rate of forest loss of all countries, but here in the zone of coniferous forest the the  
412 largest gain is observed due to agricultural abandonment (Prishchepov *et al.* 2013). The loss is maximum  
413 at the most dense areas of forest (Hansen *et al.* 2013, Table S3), this coincides with our analysis that detect  
414 an increasing risk at denser forest. This region also has a relatively low  $RS_{max}$  that means is probably near  
415 a fragmented state. A region that is similar in forest composition to EAUS1 is North America (NA1); the  
416 two main countries involved, United States and Canada, have forest dynamics mainly influenced by fire and  
417 forestry, with both regions are extensively managed for industrial wood production. North America has a  
418 higher  $RS_{max}$  than Eurasia and a positive skewness that excludes it from being near a critical transition. A  
419 possible explanation of this is that in Russia after the collapse of the Soviet Union harvest was lower due to  
420 agricultural abandonment but illegal overharvesting of high valued stands has increased in recent decades  
421 (Gauthier *et al.* 2015).

422 The analysis of  $RS_{max}$  reveals that the island of Philippines (SEAS2) seems to be an example of a critical  
423 transition from an unconnected to a connected state, i.e. from a state with high fluctuations and low  $RS_{max}$

424 to a state with low fluctuations and high  $RS_{max}$ . If we observe this pattern backwards in time, the decrease  
425 in variance increases, and negative skewness is constant, and thus the region exhibits the criteria of a critical  
426 transition (Table 1, Figure S11). The actual pattern of transition to an unfragmented state could be the  
427 result of an active intervention of the government promoting conservation and rehabilitation of protected  
428 areas, ban of logging old-growth forest, reforestation of barren areas, community-based forestry activities,  
429 and sustainable forest management in the country's production forest (Lasco *et al.* 2008). This confirms that  
430 the early warning indicators proposed here work in the correct direction. An important caveat is that the  
431 MODIS dataset does not detect if native forest is replaced by agroindustrial tree plantations like oil palms,  
432 that are among the main drivers of deforestation in this area (Malhi *et al.* 2014). To improve the estimation  
433 of forest patches, data sets as the MODIS cropland probability and others about land use, protected areas,  
434 forest type, should be incorporated (Hansen *et al.* 2014; Sexton *et al.* 2015).

435 Deforestation and fragmentation are closely related. At low levels of habitat reduction species population  
436 will decline proportionally; this can happen even when the habitat fragments retain connectivity. As habitat  
437 reduction continues, the critical threshold is approached and connectivity will have large fluctuations (Brook  
438 *et al.* 2013). This could trigger several negative synergistic effects: population fluctuations and the possibility  
439 of extinctions will rise, increasing patch isolation and decreasing connectivity (Brook *et al.* 2013). This  
440 positive feedback mechanism will be enhanced when the fragmentation threshold is reached, resulting in the  
441 loss of most habitat specialist species at a landscape scale (Pardini *et al.* 2010). Some authors have argued  
442 that since species have heterogeneous responses to habitat loss and fragmentation, and biotic dispersal is  
443 limited, the importance of thresholds is restricted to local scales or even that its existence is questionable  
444 (Brook *et al.* 2013). Fragmentation is by definition a local process that at some point produces emergent  
445 phenomena over the entire landscape, even if the area considered is infinite (Oborny *et al.* 2005). In  
446 addition, after a region's fragmentation threshold connectivity decreases, there is still a large and internally  
447 well connected patch that can maintain sensitive species (Martensen *et al.* 2012). What is the time needed  
448 for these large patches to become fragmented, and pose a real danger of extinction to a myriad of sensitive  
449 species? If a forest is already in a fragmented state, a second critical transition from forest to non-forest  
450 could happen: the desertification transition (Corrado *et al.* 2014). Considering the actual trends of habitat  
451 loss, and studying the dynamics of non-forest patches—instead of the forest patches as we did here—the risk  
452 of this kind of transition could be estimated. The simple models proposed previously could also be used to  
453 estimate if these thresholds are likely to be continuous and reversible or discontinuous and often irreversible  
454 (Weissmann & Shnerb 2016), and the degree of protection (e.g. using the set-asides strategy Banks-Leite *et*  
455 *al.* (2014)) that would be necessary to stop this trend.

456 The effectiveness of landscape management is related to the degree of fragmentation, and the criteria to direct  
457 reforestation efforts could be focused on regions near a transition (Oborny *et al.* 2007). Regions that are in  
458 an unconnected state require large efforts to recover a connected state, but regions that are near a transition  
459 could be easily pushed to a connected state; feedbacks due to facilitation mechanisms might help to maintain  
460 this state. Crossing the fragmentation critical point in forests could have negative effects on biodiversity and  
461 ecosystem services (Haddad *et al.* 2015), but it could also produce feedback loops at different levels of the  
462 biological hierarchy. This means that a critical transition produced at a continental scale could have effects  
463 at the level of communities, food webs, populations, phenotypes and genotypes (Barnosky *et al.* 2012). All  
464 these effects interact with climate change, thus there is a potential production of cascading effects that could  
465 lead to an abrupt climate change with potentially large ecological and economic impact (Alley *et al.* 2003).

466 Therefore, even if critical thresholds are reached only in some forest regions at a continental scale, a cascading  
467 effect with global consequences could still be produced (Reyer *et al.* 2015). The risk of such event will be  
468 higher if the dynamics of separate continental regions are coupled (Lenton & Williams 2013). At least  
469 three of the regions defined here are considered tipping elements of the earth climate system that could be  
470 triggered during this century (Lenton *et al.* 2008). These were defined as policy relevant tipping elements  
471 so that political decisions could determine whether the critical value is reached or not. Thus using the  
472 criteria proposed here could be used as a more sensitive system to evaluate the closeness of a tipping point  
473 at a continental scale, but the same criteria could also be used to evaluate local problems at smaller areas.  
474 Further improvements will produce quantitative predictions about the temporal horizon where these critical  
475 transitions could produce significant changes in the studied systems.

## 476 Supporting information

### 477 Appendix

478 *Table S1:* Mean power-law exponent and Bootstrapped 95% confidence intervals by threshold.

479 *Table S2:* Mean power-law exponent and Bootstrapped 95% confidence intervals across thresholds by region  
480 and year.

481 *Table S3:* Mean total patch area; largest patch  $S_{max}$  in km<sup>2</sup>; largest patch proportional to total patch area  
482  $RS_{max}$  and 95% bootstrapped confidence interval of  $RS_{max}$ , by region and thresholds, averaged across years

483 *Table S4:* Model selection for distributions of fluctuation of largest patch  $\Delta S_{max}$  and largest patch relative  
484 to total forest area  $\Delta RS_{max}$ .

- 485 *Table S5*: Quantil regressions of the fluctuations of the largest patch vs year, for 10% and 90% quantils at  
 486 different pixel thresholds.
- 487 *Table S6*: Unbiased estimation of Skewness of fluctuations of the largest patch  $\Delta S_{max}$  and fluctuations  
 488 relative to total forest area  $\Delta RS_{max}$ .
- 489 *Figure S1*: Regions for Africa: Mainland (AF1), Madagascar (AF2).
- 490 *Figure S2*: Regions for Eurasia: Mainland (EUAS1), Japan (EUAS2), Great Britain (EUAS3).
- 491 *Figure S3*: Regions for North America: Mainland (NA1), Newfoundland (NA5).
- 492 *Figure S4*: Regions for Australia and islands: Australia mainland (OC1), New Guinea (OC2),  
 493 Malaysia/Kalimantan (OC3), Sumatra (OC4), Sulawesi (OC5), New Zealand south island (OC6),  
 494 Java (OC7), New Zealand north island (OC8).
- 495 *Figure S5*: Regions for South America: Tropical and subtropical forest up to Mexico (SAST1), Cuba  
 496 (SAST2), South America Temperate forest (SAT1).
- 497 *Figure S6*: Regions for Southeast Asia: Mainland (SEAS1), Philippines (SEAS2).
- 498 *Figure S7*: Proportion of best models selected for patch size distributions using the Akaike criterion.
- 499 *Figure S8*: Power law exponents for forest patch distributions by year for all regions.
- 500 *Figure S9*: Average largest patch relative to total forest area  $RS_{max}$  by threshold, for all regions.
- 501 *Figure S10*: Largest patch relative to total forest area  $RS_{max}$  by year at 40% threshold, for regions with  
 502 total forest area less than  $10^7 \text{ km}^2$ .
- 503 *Figure S11*: Fluctuations of largest patch relative to total forest area  $RS_{max}$  for regions with total forest  
 504 area less than  $10^7 \text{ km}^2$  by year and threshold.

## 505 Data Accessibility

- 506 The MODIS VCF product is freely available from NASA at <https://search.earthdata.nasa.gov/>. Csv text file  
 507 with model fits for patch size distribution, and model selection for all the regions; Gif Animations of a forest  
 508 model percolation; Gif animations of largest patches; patch size files for all years and regions used here; and all  
 509 the R, Python and Matlab scripts are available at figshare <http://dx.doi.org/10.6084/m9.figshare.4263905>.

510 **Acknowledgments**

511 LAS and SRD are grateful to the National University of General Sarmiento for financial support. We want to  
512 thank Jordi Bascompte, Nara Guisoni, Fernando Momo, and two anonymous reviewers for their comments  
513 and discussions that greatly improved the manuscript. This work was partially supported by a grant from  
514 CONICET (PIO 144-20140100035-CO).

515 **References**

- 516 Alley, R.B., Marotzke, J., Nordhaus, W.D., Overpeck, J.T., Peteet, D.M. & Pielke, R.A. *et al.* (2003).  
517 Abrupt Climate Change. *Science*, 299, 2005–2010.
- 518 Allington, G.R.H. & Valone, T.J. (2010). Reversal of desertification: The role of physical and chemical soil  
519 properties. *Journal of Arid Environments*, 74, 973–977.
- 520 Alstott, J., Bullmore, E. & Plenz, D. (2014). powerlaw: A Python Package for Analysis of Heavy-Tailed  
521 Distributions. *PLOS ONE*, 9, e85777.
- 522 Angelsen, A. (2010). Policies for reduced deforestation and their impact on agricultural production. *Pro-*  
523 *ceedings of the National Academy of Sciences*, 107, 19639–19644.
- 524 Banks-Leite, C., Pardini, R., Tambosi, L.R., Pearse, W.D., Bueno, A.A. & Bruscagin, R.T. *et al.* (2014).  
525 Using ecological thresholds to evaluate the costs and benefits of set-asides in a biodiversity hotspot. *Science*,  
526 345, 1041–1045.
- 527 Barnosky, A.D., Hadly, E.A., Bascompte, J., Berlow, E.L., Brown, J.H. & Fortelius, M. *et al.* (2012).  
528 Approaching a state shift in Earth’s biosphere. *Nature*, 486, 52–58.
- 529 Bascompte, J. & Solé, R.V. (1996). Habitat fragmentation and extinction threholds in spatially explicit  
530 models. *Journal of Animal Ecology*, 65, 465–473.
- 531 Bazant, M.Z. (2000). Largest cluster in subcritical percolation. *Physical Review E*, 62, 1660–1669.
- 532 Belward, A.S. (1996). *The IGBP-DIS Global 1 Km Land Cover Data Set “DISCover”: Proposal and*  
533 *Implementation Plans : Report of the Land Recover Working Group of IGBP-DIS*. IGBP-dis working paper.  
534 IGBP-DIS Office.
- 535 Benedetti-Cecchi, L., Tamburello, L., Maggi, E. & Bulleri, F. (2015). Experimental Perturbations Modify

- 536 the Performance of Early Warning Indicators of Regime Shift. *Current biology*, 25, 1867–1872.
- 537 Bestelmeyer, B.T., Duniway, M.C., James, D.K., Burkett, L.M. & Havstad, K.M. (2013). A test of critical  
538 thresholds and their indicators in a desertification-prone ecosystem: more resilience than we thought. *Ecology*  
539 *Letters*, 16, 339–345.
- 540 Bestelmeyer, B.T., Ellison, A.M., Fraser, W.R., Gorman, K.B., Holbrook, S.J. & Laney, C.M. *et al.* (2011).  
541 Analysis of abrupt transitions in ecological systems. *Ecosphere*, 2, 129.
- 542 Boettiger, C. & Hastings, A. (2012). Quantifying limits to detection of early warning for critical transitions.  
543 *Journal of The Royal Society Interface*, 9, 2527–2539.
- 544 Bonan, G.B. (2008). Forests and Climate Change: Forcings, Feedbacks, and the Climate Benefits of Forests.  
545 *Science*, 320, 1444–1449.
- 546 Botet, R. & Ploszajczak, M. (2004). Correlations in Finite Systems and Their Universal Scaling Properties.  
547 In: *Nonequilibrium physics at short time scales: Formation of correlations* (ed. Morawetz, K.). Springer-  
548 Verlag, Berlin Heidelberg, pp. 445–466.
- 549 Brook, B.W., Ellis, E.C., Perring, M.P., Mackay, A.W. & Blomqvist, L. (2013). Does the terrestrial biosphere  
550 have planetary tipping points? *Trends in Ecology & Evolution*.
- 551 Burnham, K. & Anderson, D.R. (2002). *Model selection and multi-model inference: A practical information-  
552 theoretic approach*. 2nd. edn. Springer-Verlag, New York.
- 553 Canfield, D.E., Glazer, A.N. & Falkowski, P.G. (2010). The Evolution and Future of Earth’s Nitrogen Cycle.  
554 *Science*, 330, 192–196.
- 555 Carpenter, S.R., Cole, J.J., Pace, M.L., Batt, R., Brock, W.A. & Cline, T. *et al.* (2011). Early Warnings of  
556 Regime Shifts: A Whole-Ecosystem Experiment. *Science*, 332, 1079–1082.
- 557 Clauset, A., Shalizi, C. & Newman, M. (2009). Power-Law Distributions in Empirical Data. *SIAM Review*,  
558 51, 661–703.
- 559 Corrado, R., Cherubini, A.M. & Pennetta, C. (2014). Early warning signals of desertification transitions in  
560 semiarid ecosystems. *Physical Review E - Statistical, Nonlinear, and Soft Matter Physics*, 90, 62705.
- 561 Crawley, M.J. (2012). *The R Book*. 2nd. edn. Wiley, Hoboken, NJ, USA.
- 562 Crowther, T.W., Glick, H.B., Covey, K.R., Bettigole, C., Maynard, D.S. & Thomas, S.M. *et al.* (2015).

- 563 Mapping tree density at a global scale. *Nature*, 525, 201–205.
- 564 Dai, L., Vorselen, D., Korolev, K.S. & Gore, J. (2012). Generic Indicators for Loss of Resilience Before a  
565 Tipping Point Leading to Population Collapse. *Science*, 336, 1175–1177.
- 566 DiMiceli, C., Carroll, M., Sohlberg, R., Huang, C., Hansen, M. & Townshend, J. (2015). Annual Global  
567 Automated MODIS Vegetation Continuous Fields (MOD44B) at 250 m Spatial Resolution for Data Years  
568 Beginning Day 65, 2000 - 2014, Collection 051 Percent Tree Cover, University of Maryland, College Park,  
569 MD, USA.
- 570 Drake, J.M. & Griffen, B.D. (2010). Early warning signals of extinction in deteriorating environments.  
571 *Nature*, 467, 456–459.
- 572 Efron, B. & Tibshirani, R.J. (1994). *An Introduction to the Bootstrap*. Chapman & hall/crc monographs on  
573 statistics & applied probability. Taylor & Francis, New York.
- 574 Filotas, E., Parrott, L., Burton, P.J., Chazdon, R.L., Coates, K.D. & Coll, L. *et al.* (2014). Viewing forests  
575 through the lens of complex systems science. *Ecosphere*, 5, 1–23.
- 576 Foley, J.A., Ramankutty, N., Brauman, K.A., Cassidy, E.S., Gerber, J.S. & Johnston, M. *et al.* (2011).  
577 Solutions for a cultivated planet. *Nature*, 478, 337–342.
- 578 Folke, C., Jansson, Å., Rockström, J., Olsson, P., Carpenter, S.R. & Iii, F.S.C. *et al.* (2011). Reconnecting  
579 to the Biosphere. *AMBIO*, 40, 719–738.
- 580 Fung, T., O'Dwyer, J.P., Rahman, K.A., Fletcher, C.D. & Chisholm, R.A. (2016). Reproducing static and  
581 dynamic biodiversity patterns in tropical forests: the critical role of environmental variance. *Ecology*, 97,  
582 1207–1217.
- 583 Gardner, R.H. & Urban, D.L. (2007). Neutral models for testing landscape hypotheses. *Landscape Ecology*,  
584 22, 15–29.
- 585 Gastner, M.T., Oborny, B., Zimmermann, D.K. & Pruessner, G. (2009). Transition from Connected to Frag-  
586 mented Vegetation across an Environmental Gradient: Scaling Laws in Ecotone Geometry. *The American  
587 Naturalist*, 174, E23–E39.
- 588 Gauthier, S., Bernier, P., Kuuluvainen, T., Shvidenko, A.Z. & Schepaschenko, D.G. (2015). Boreal forest  
589 health and global change. *Science*, 349, 819 LP–822.
- 590 Gilman, S.E., Urban, M.C., Tewksbury, J., Gilchrist, G.W. & Holt, R.D. (2010). A framework for community

- 591 interactions under climate change. *Trends in Ecology & Evolution*, 25, 325–331.
- 592 Goldstein, M.L., Morris, S.A. & Yen, G.G. (2004). Problems with fitting to the power-law distribution. *The*  
593 *European Physical Journal B - Condensed Matter and Complex Systems*, 41, 255–258.
- 594 Haddad, N.M., Brudvig, L.a., Clobert, J., Davies, K.F., Gonzalez, A. & Holt, R.D. *et al.* (2015). Habitat  
595 fragmentation and its lasting impact on Earth's ecosystems. *Science Advances*, 1, 1–9.
- 596 Hansen, M., Potapov, P., Margono, B., Stehman, S., Turubanova, S. & Tyukavina, A. (2014). Response to  
597 Comment on “High-resolution global maps of 21st-century forest cover change”. *Science*, 344, 981.
- 598 Hansen, M.C., Potapov, P.V., Moore, R., Hancher, M., Turubanova, S.A. & Tyukavina, A. *et al.* (2013).  
599 High-Resolution Global Maps of 21st-Century Forest Cover Change. *Science*, 342, 850–853.
- 600 Hantson, S., Pueyo, S. & Chuvieco, E. (2015). Global fire size distribution is driven by human impact and  
601 climate. *Global Ecology and Biogeography*, 24, 77–86.
- 602 Harris, T.E. (1974). Contact interactions on a lattice. *The Annals of Probability*, 2, 969–988.
- 603 Hartigan, J.A. & Hartigan, P.M. (1985). The Dip Test of Unimodality. *The Annals of Statistics*, 13, 70–84.
- 604 Hastings, A. & Wysham, D.B. (2010). Regime shifts in ecological systems can occur with no warning. *Ecology*  
605 *Letters*, 13, 464–472.
- 606 He, F. & Hubbell, S. (2003). Percolation Theory for the Distribution and Abundance of Species. *Physical*  
607 *Review Letters*, 91, 198103.
- 608 Heffernan, J.B., Soranno, P.A., Angilletta, M.J., Buckley, L.B., Gruner, D.S. & Keitt, T.H. *et al.* (2014).  
609 Macrosystems ecology: understanding ecological patterns and processes at continental scales. *Frontiers in*  
610 *Ecology and the Environment*, 12, 5–14.
- 611 Hinrichsen, H. (2000). Non-equilibrium critical phenomena and phase transitions into absorbing states.  
612 *Advances in Physics*, 49, 815–958.
- 613 Hirota, M., Holmgren, M., Nes, E.H.V. & Scheffer, M. (2011). Global Resilience of Tropical Forest and  
614 Savanna to Critical Transitions. *Science*, 334, 232–235.
- 615 Irvine, M.A., Bull, J.C. & Keeling, M.J. (2016). Aggregation dynamics explain vegetation patch-size distri-  
616 butions. *Theoretical Population Biology*, 108, 70–74.
- 617 Keitt, T.H., Urban, D.L. & Milne, B.T. (1997). Detecting critical scales in fragmented landscapes. *Conser-*

- 618 *vation Ecology*, 1, 4.
- 619 Kéfi, S., Guttal, V., Brock, W.A., Carpenter, S.R., Ellison, A.M. & Livina, V.N. *et al.* (2014). Early  
620 Warning Signals of Ecological Transitions: Methods for Spatial Patterns. *PLoS ONE*, 9, e92097.
- 621 Kéfi, S., Rietkerk, M., Alados, C.L., Pueyo, Y., Papanastasis, V.P. & ElAich, A. *et al.* (2007). Spatial  
622 vegetation patterns and imminent desertification in Mediterranean arid ecosystems. *Nature*, 449, 213–217.
- 623 Kitzberger, T., Aráoz, E., Gowda, J.H., Mermoz, M. & Morales, J.M. (2012). Decreases in Fire Spread Prob-  
624 ability with Forest Age Promotes Alternative Community States, Reduced Resilience to Climate Variability  
625 and Large Fire Regime Shifts. *Ecosystems*, 15, 97–112.
- 626 Koenker, R. (2016). quantreg: Quantile Regression.
- 627 Lasco, R.D., Pulhin, F.B., Cruz, R.V.O., Pulhin, J.M., Roy, S.S.N. & Sanchez, P.A.J. (2008). Forest  
628 responses to changing rainfall in the Philippines. In: *Climate change and vulnerability* (eds. Leary, N.,  
629 Conde, C. & Kulkarni, J.). Earthscan, London, pp. 49–66.
- 630 Leibold, M.A. & Norberg, J. (2004). Biodiversity in metacommunities: Plankton as complex adaptive  
631 systems? *Limnology and Oceanography*, 49, 1278–1289.
- 632 Lenton, T.M. & Williams, H.T.P. (2013). On the origin of planetary-scale tipping points. *Trends in Ecology  
& Evolution*, 28, 380–382.
- 634 Lenton, T.M., Held, H., Kriegler, E., Hall, J.W., Lucht, W. & Rahmstorf, S. *et al.* (2008). Tipping elements  
635 in the Earth's climate system. *Proceedings of the National Academy of Sciences*, 105, 1786–1793.
- 636 Limpert, E., Stahel, W.A. & Abbt, M. (2001). Log-normal Distributions across the Sciences: Keys and  
637 CluesOn the charms of statistics, and how mechanical models resembling gambling machines offer a link to  
638 a handy way to characterize log-normal distributions, which can provide deeper insight into var. *BioScience*,  
639 51, 341–352.
- 640 Loehle, C., Li, B.-L. & Sundell, R.C. (1996). Forest spread and phase transitions at forest-prairie ecotones  
641 in Kansas, U.S.A. *Landscape Ecology*, 11, 225–235.
- 642 Malhi, Y., Gardner, T.A., Goldsmith, G.R., Silman, M.R. & Zelazowski, P. (2014). Tropical Forests in the  
643 Anthropocene. *Annual Review of Environment and Resources*, 39, 125–159.
- 644 Manor, A. & Shnerb, N.M. (2008). Origin of pareto-like spatial distributions in ecosystems. *Physical Review  
Letters*, 101, 268104.
- 646 Martensen, A.C., Ribeiro, M.C., Banks-Leite, C., Prado, P.I. & Metzger, J.P. (2012). Associations of Forest

- 647 Cover, Fragment Area, and Connectivity with Neotropical Understory Bird Species Richness and Abundance.
- 648 *Conservation Biology*, 26, 1100–1111.
- 649 McKenzie, D. & Kennedy, M.C. (2012). Power laws reveal phase transitions in landscape controls of fire
- 650 regimes. *Nat Commun*, 3, 726.
- 651 Mitchell, M.G.E., Suarez-Castro, A.F., Martinez-Harms, M., Maron, M., McAlpine, C. & Gaston, K.J. *et al.*
- 652 (2015). Reframing landscape fragmentation's effects on ecosystem services. *Trends in Ecology & Evolution*,
- 653 30, 190–198.
- 654 Naito, A.T. & Cairns, D.M. (2015). Patterns of shrub expansion in Alaskan arctic river corridors suggest
- 655 phase transition. *Ecology and Evolution*, 5, 87–101.
- 656 Newman, M.E.J. (2005). Power laws, Pareto distributions and Zipf's law. *Contemporary Physics*, 46, 323–
- 657 351.
- 658 Oborny, B., Meszéna, G. & Szabó, G. (2005). Dynamics of Populations on the Verge of Extinction. *Oikos*,
- 659 109, 291–296.
- 660 Oborny, B., Szabó, G. & Meszéna, G. (2007). Survival of species in patchy landscapes: percolation in space
- 661 and time. In: *Scaling biodiversity*. Cambridge University Press, pp. 409–440.
- 662 Ochoa-Quintero, J.M., Gardner, T.A., Rosa, I., de Barros Ferraz, S.F. & Sutherland, W.J. (2015). Thresholds
- 663 of species loss in Amazonian deforestation frontier landscapes. *Conservation Biology*, 29, 440–451.
- 664 Ódor, G. (2004). Universality classes in nonequilibrium lattice systems. *Reviews of Modern Physics*, 76,
- 665 663–724.
- 666 Pardini, R., Bueno, A. de A., Gardner, T.A., Prado, P.I. & Metzger, J.P. (2010). Beyond the Fragmentation
- 667 Threshold Hypothesis: Regime Shifts in Biodiversity Across Fragmented Landscapes. *PLoS ONE*, 5, e13666.
- 668 Potapov, P., Hansen, M.C., Stehman, S.V., Loveland, T.R. & Pittman, K. (2008a). Combining MODIS
- 669 and Landsat imagery to estimate and map boreal forest cover loss. *Remote Sensing of Environment*, 112,
- 670 3708–3719.
- 671 Potapov, P., Yaroshenko, A., Turubanova, S., Dubinin, M., Laestadius, L. & Thies, C. *et al.* (2008b).
- 672 Mapping the world's intact forest landscapes by remote sensing. *Ecology and Society*, 13.
- 673 Prishchepov, A.V., Müller, D., Dubinin, M., Baumann, M. & Radeloff, V.C. (2013). Determinants of
- 674 agricultural land abandonment in post-Soviet European Russia. *Land Use Policy*, 30, 873–884.
- 675 Pueyo, S., de Alencastro Graça, P.M.L., Barbosa, R.I., Cots, R., Cardona, E. & Fearnside, P.M. (2010).

- 676 Testing for criticality in ecosystem dynamics: the case of Amazonian rainforest and savanna fire. *Ecology*  
677 *Letters*, 13, 793–802.
- 678 R Core Team. (2015). R: A Language and Environment for Statistical Computing.
- 679 Reyer, C.P.O., Rammig, A., Brouwers, N. & Langerwisch, F. (2015). Forest resilience, tipping points and  
680 global change processes. *Journal of Ecology*, 103, 1–4.
- 681 Rockstrom, J., Steffen, W., Noone, K., Persson, A., Chapin, F.S. & Lambin, E.F. *et al.* (2009). A safe  
682 operating space for humanity. *Nature*, 461, 472–475.
- 683 Rooij, M.M.J.W. van, Nash, B., Rajaraman, S. & Holden, J.G. (2013). A Fractal Approach to Dynamic  
684 Inference and Distribution Analysis. *Frontiers in Physiology*, 4.
- 685 Rudel, T.K., Coomes, O.T., Moran, E., Achard, F., Angelsen, A. & Xu, J. *et al.* (2005). Forest transitions:  
686 towards a global understanding of land use change. *Global Environmental Change*, 15, 23–31.
- 687 Saravia, L.A. & Momo, F.R. (2017). Biodiversity collapse and early warning indicators in a spatial phase  
688 transition between neutral and niche communities. *PeerJ PrePrints*, 5, e1589v4.
- 689 Scanlon, T.M., Caylor, K.K., Levin, S.A. & Rodriguez-iturbe, I. (2007). Positive feedbacks promote power-  
690 law clustering of Kalahari vegetation. *Nature*, 449, 209–212.
- 691 Scheffer, M., Bascompte, J., Brock, W.A., Brovkin, V., Carpenter, S.R. & Dakos, V. *et al.* (2009). Early-  
692 warning signals for critical transitions. *Nature*, 461, 53–59.
- 693 Scheffer, M., Walker, B., Carpenter, S., Foley, J. a, Folke, C. & Walker, B. (2001). Catastrophic shifts in  
694 ecosystems. *Nature*, 413, 591–596.
- 695 Seidler, T.G. & Plotkin, J.B. (2006). Seed Dispersal and Spatial Pattern in Tropical Trees. *PLoS Biology*,  
696 4, e344.
- 697 Sexton, J.O., Noojipady, P., Song, X.-P., Feng, M., Song, D.-X. & Kim, D.-H. *et al.* (2015). Conservation  
698 policy and the measurement of forests. *Nature Climate Change*, 6, 192–196.
- 699 Sexton, J.O., Song, X.-P., Feng, M., Noojipady, P., Anand, A. & Huang, C. *et al.* (2013). Global, 30-m  
700 resolution continuous fields of tree cover: Landsat-based rescaling of MODIS vegetation continuous fields  
701 with lidar-based estimates of error. *International Journal of Digital Earth*, 6, 427–448.
- 702 Solé, R.V. (2011). *Phase Transitions*. Primers in complex systems. Princeton University Press.
- 703 Solé, R.V. & Bascompte, J. (2006). *Self-organization in complex ecosystems*. Princeton University Press,

- 704 New Jersey, USA.
- 705 Solé, R.V., Alonso, D. & Mckane, A. (2002). Self-organized instability in complex ecosystems. *Philosophical  
706 transactions of the Royal Society of London. Series B, Biological sciences*, 357, 667–681.
- 707 Solé, R.V., Alonso, D. & Saldaña, J. (2004). Habitat fragmentation and biodiversity collapse in neutral  
708 communities. *Ecological Complexity*, 1, 65–75.
- 709 Solé, R.V., Bartumeus, F. & Gamarra, J.G.P. (2005). Gap percolation in rainforests. *Oikos*, 110, 177–185.
- 710 Staal, A., Dekker, S.C., Xu, C. & Nes, E.H. van. (2016). Bistability, Spatial Interaction, and the Distribution  
711 of Tropical Forests and Savannas. *Ecosystems*, 19, 1080–1091.
- 712 Stauffer, D. & Aharony, A. (1994). *Introduction To Percolation Theory*. Taylor & Francis, London.
- 713 Taubert, F., Fischer, R., Groeneveld, J., Lehmann, S., Müller, M.S. & Rödig, E. et al. (2018). Global  
714 patterns of tropical forest fragmentation. *Nature*.
- 715 Vasilakopoulos, P. & Marshall, C.T. (2015). Resilience and tipping points of an exploited fish population  
716 over six decades. *Global Change Biology*, 21, 1834–1847.
- 717 Villa Martín, P., Bonachela, J.A. & Muñoz, M.A. (2014). Quenched disorder forbids discontinuous transitions  
718 in nonequilibrium low-dimensional systems. *Physical Review E*, 89, 12145.
- 719 Villa Martín, P., Bonachela, J.A., Levin, S.A. & Muñoz, M.A. (2015). Eluding catastrophic shifts. *Proceed-  
720 ings of the National Academy of Sciences*, 112, E1828–E1836.
- 721 Viña, A., McConnell, W.J., Yang, H., Xu, Z. & Liu, J. (2016). Effects of conservation policy on China's  
722 forest recovery. *Science Advances*, 2, e1500965.
- 723 Vuong, Q.H. (1989). Likelihood Ratio Tests for Model Selection and Non-Nested Hypotheses. *Econometrica*,  
724 57, 307–333.
- 725 Weerman, E.J., Van Belzen, J., Rietkerk, M., Temmerman, S., Kéfi, S. & Herman, P.M.J. et al. (2012).  
726 Changes in diatom patch-size distribution and degradation in a spatially self-organized intertidal mudflat  
727 ecosystem. *Ecology*, 93, 608–618.
- 728 Weissmann, H. & Shnerb, N.M. (2016). Predicting catastrophic shifts. *Journal of Theoretical Biology*, 397,  
729 128–134.
- 730 Wuyts, B., Champneys, A.R. & House, J.I. (2017). Amazonian forest-savanna bistability and human impact.

- 731 *Nature Communications*, 8, 15519.
- 732 Xu, C., Hantson, S., Holmgren, M., Nes, E.H. van, Staal, A. & Scheffer, M. (2016). Remotely sensed canopy  
733 height reveals three pantropical ecosystem states. *Ecology*, 97, 2518–2521.
- 734 Zhang, J.Y., Wang, Y., Zhao, X., Xie, G. & Zhang, T. (2005). Grassland recovery by protection from grazing  
735 in a semi-arid sandy region of northern China. *New Zealand Journal of Agricultural Research*, 48, 277–284.
- 736 Zinck, R.D. & Grimm, V. (2009). Unifying wildfire models from ecology and statistical physics. *The  
737 American naturalist*, 174, E170–85.